

Radar

IMPROVED SEVERE STORM WARNINGS USING DOPPLER RADAR

Rodger A. Brown (1)
and Vincent T. Wood (2)

National Severe Storms Laboratory
Norman, Oklahoma 73069

ABSTRACT

Research data collected by the National Severe Storms Laboratory's Doppler radars and operational tests conducted during the Joint Doppler Operational Project reveal the severe storm detection capability of 10-cm wavelength Doppler radars. Severe storm identification is based on the presence of the Doppler velocity signature of a mesocyclone -- a circulation that appears on conventional radar scopes as a hook echo.

1. INTRODUCTION

There has been increasing discussion recently about replacing the nation's aging weather radars with a network that has Doppler capability (e.g., Grebe (3)). Why are claims being made that a Doppler radar will do a better job than a conventional radar in detecting severe thunderstorms? To answer this question, we need to explore what has been taking place during the past 15 to 20 years.

We know that power scattered back to a conventional (incoherent) radar is a function of the size and number concentration of precipitation particles in the storm. A Doppler radar has the same capability -- and more. Being coherent, a Doppler radar also is able to sense the very slight frequency shift (Doppler effect) caused by the movement of precipitation particles relative to the radar. The frequency shift at each location in the storm then can be converted into a Doppler velocity value.

It is important to note that a Doppler radar senses only the component of motion in the direction the radar is pointing. For example, when the radar is pointing north, only the north-south component of the wind is measured; the east-west component cannot be detected. Similarly, when the radar is pointing toward the northeast, the northeast-southwest component is fully sensed while the northwest-southeast component is not sensed at all. We discuss some specific examples in the next section.

During the latter half of the 1960's, Doppler radar investigators noted that information about the horizontal flow fields in

thunderstorms could be deduced from single Doppler velocity data (e.g., Easterbrook (4), Donaldson (5), Peace and Brown (6), Donaldson et al. (7), Lhermitte (8)). Recognizing, however, that unique flow fields cannot be determined from such data, Donaldson (9) proposed a set of criteria for helping to distinguish mesoscale vortices (mesocyclones) from regions of azimuthal shear (that is, shear across the radar viewing direction). In effect, the criteria designate an azimuthal shear region to be a vortex when the shear region (a) persists for at least half the time period required for one vortex rotation, (b) extends vertically a distance greater than the shear diameter, (c) does not change its basic pattern during a viewing direction change of approximately 45° and (d) when the azimuthal (angular) width of the shear regions is in a position relative to the radar where the viewing direction changes by less than 45° during a major portion of the feature's lifetime. Therefore one usually applies only the other three criteria.

2. DOPPLER VELOCITY SIGNATURES OF MESOCYCLONES AND DIVERGENCE AREAS

We start with a discussion of single Doppler velocity signatures that help identify severe thunderstorms. Two horizontal flow fields that easily are recognized through Doppler velocity "signatures" are rotation and convergence/divergence. Examples of these fields are shown in Fig. 1; the basic features are zero velocity at the center and maximum velocity (bold arrows) at a radius R from the center.

There are a number of different models that one can use to describe the variation

of velocity with radius. We choose a simple model -- called the Rankine combined velocity profile (Fig. 2) -- that approximates the basic features observed in the atmosphere. This profile consists of two distinct velocity (v) distributions. The inner portion of the profile increases linearly with distance (r) from the center

$$v = C_1 r \quad (r \leq R) \quad (1)$$

In the outer portion, velocity change is inversely proportional to distance from the center

$$v = C_2 r \quad (r > R) \quad (2)$$

The inner part of the profile will be referred to as the core region with R being the core radius. The maximum velocity, V_x , in the profile occurs at the core radius. Once R and V_x are specified, the entire profile can be determined using the constants

$$C_1 = V_x/R \quad (\text{within core region, } r \leq R) \quad (3)$$

$$C_2 = V_x/R \quad (\text{within core region, } r > R) \quad (4)$$

2.a. Mesocyclone Signature

The combined velocity profile originally was developed to describe axisymmetric vortices (e.g., Rankine (10)). For a vortex, v_t represents tangential (rotational) velocity and V_t represents peak tangential velocity. Since tangential velocity is modeled to increase linearly with radius within the core region ($r \leq R$), the core rotates like a vertical solid cylinder (having a circular horizontal cross-section). The cylinder thus represents the driving force that keeps the surrounding fluid (water or air) rotating; fluid tangential velocity changes inversely with distance from the rotation center.

By analogy, a fluid vortex can be thought of as having a core that rotates as if it were a solid. This model is a good first approximation for describing atmospheric vortices ranging in size from dust devils to hurricanes. The key parameters needed to specify a vortex in nature are the core radius and the maximum tangential velocity. These two parameters form the basis for the single Doppler velocity signature of a mesocyclone.

Figure 3 shows a horizontal scan through a vortex (thick circular lines) rotating around a vertical axis and the associated single Doppler velocity pattern (thinner lines -- lines having constant Doppler velocity values). A Doppler radar is assumed to be located a considerable distance due south of the vortex center. Since a Doppler radar senses only the component of flow in the radar viewing direction, the heavy dashed line represents ze-

ro Doppler velocity because flow everywhere along the line is perpendicular to the viewing direction. To the right of the line, flow is away from the radar (thin solid contours) and flow on the left is toward the radar (thin dashed contours). Whereas a Doppler radar senses none of the flow when viewing a vortex through the circulation center, it senses the complete flow on both sides of the center where flow is directly toward or away from the radar. The arrows either side of center represent the core radius (R) where the full value of the peak tangential velocity (V_t) is measured.

Therefore the single Doppler velocity signature of a mesocyclone (or any vortex) has a pattern that is symmetric about the radar viewing direction and has peak values (V_t) of opposite sign at the core radius (R) either side of the circulation center. If the vortex is moving and/or is embedded in a uniform horizontal flow field, the circulation no longer will be circular but the vortex signature pattern will remain unchanged; the only difference will be that the contour lines will have different values and the center contour no longer will have a Doppler velocity value of zero.

A mesocyclone is a rotating column (10 to 15 km diameter) within a severe thunderstorm that usually is associated with the storm's updraft. Looking in the direction of storm motion, the mesocyclone is found on the right rear flank. Under ideal conditions, the mesocyclone appears as a "hook echo" on a conventional radar display. If a bounded weak echo region -- indicating a very strong updraft -- appears in the radar reflectivity pattern, it usually coincides with the mesocyclone.

An example of a mesocyclone signature near cloud base is shown in Fig. 4. During the 45-minute period ending 5 minutes before the data time, the storm caused extensive damage due to very large hail, strong winds and at least 5 short-lived tornadoes. At data time, the storm was becoming nonsevere with heavy rain at the surface within the mesocyclone. Negative Doppler velocities represent flow toward the radar and positive velocities are flow away; storm motion has been subtracted, so velocities are those as seen by an observer moving with the storm. The signature is located about 80 km south-southeast of the Norman Doppler radar. The average Doppler velocity value across the signature of about -6 m s^{-1} represents a component of southerly environmental winds near cloud base.

2.b. Divergence Signature

The Rankine combined profile also can be used to model axisymmetric divergence/

convergence areas (Fig. 1b). In this case, v_r represents radial velocities flowing directly inward toward or outward from the center of the model; V_r is the peak radial velocity. Since radial velocity changes at a constant rate with increasing radius in the core region ($r \leq R$), horizontal divergence is constant within the core.

A model radial flow field and the corresponding single Doppler velocity pattern is shown in Fig. 5. Note that the divergence signature is the same as a mesocyclone signature that has been rotated counterclockwise by 90°. Here the zero line is perpendicular to the radar viewing direction because the radar does not sense motion toward the left or right of the divergence center. Maximum flow toward and away from the radar (short arrows) is V_r measured along the viewing direction that passes through the divergence center; these peak velocities occur at the core radius.

An example of a divergence signature near storm top is found in Fig. 6. In this case, the radar (located above the top of the figure) is about 145 km north of the signature center. The average of the Doppler velocity maxima (located near the closest and farthest edges of the radar echo) is 77 m s⁻¹. If we assume that the peak values should be +77 m s⁻¹, the measurements suggest that a Doppler velocity component of -11 m s⁻¹ -- representing the component of storm motion and environmental winds at the data level -- has been added to the pure divergence signature.

3. COMPUTATION OF VORTICITY, DIVERGENCE AND VERTICAL VELOCITY FROM SINGLE DOPPLER VELOCITY DATA

The mathematical definitions of vertical vorticity component (5) and horizontal divergence ($\vec{\nabla} \cdot \vec{V}$) in an exisymmetric coordinate system (e.g., Spiegel (13), pp. 153-154) are

$$\zeta = \frac{\partial v_t}{\partial r} + \frac{v_t}{r} \quad (5)$$

$$\vec{\nabla} \cdot \vec{V} = \frac{\partial v_r}{\partial r} + \frac{v_r}{r} \quad (6)$$

where the arrow indicates a vector quantity, $\vec{\nabla}$ is the vector differential operator and \vec{V} is the horizontal wind vector. Substituting Eqs. (1) and (3) into (5) and (6), we find that within the core region

$$\zeta = \frac{2 V_t}{R} \quad (7)$$

$$\vec{\nabla} \cdot \vec{V} = \frac{2 V_r}{R} \quad (r \leq R) \quad (8)$$

Outside the core region, substituting Eqs. (2) and (4) into (5) and (6), we find that

$$\begin{aligned} \zeta &= 0 \\ \vec{\nabla} \cdot \vec{V} &= 0 \end{aligned} \quad (r > R) \quad (9)$$

(10)

For one who is not familiar with the implications of the Rankine combined velocity profile, the results of Eqs. (7)-(10) may be surprising: vorticity and divergence are constant within the core region and zero outside. Constant vorticity in the core should be expected since the core rotates like a solid. Even though the fluid outside the core is rotating (e.g., Fig. 1a), the mathematical quantity called vorticity is zero because the two terms in Eq. (5) have the same magnitude but have opposite signs, cancelling each other. Constant divergence within the core region implies uniform vertical velocity within the core.

3.a. Derivation of General Equations

So far, we have discussed only those situations where pure vorticity (Fig. 3) or pure divergence (Fig. 5) are present. In reality, some combination of the two quantities usually exist. If we assume that the core radii and peak velocities for the two quantities are equal, Eq. (7) and (8) can be modified for those situations where both vorticity and divergence are present.

For an orientation of the Doppler velocity pattern other than pure rotation or pure convergence/divergence, peak Doppler velocity values at the core radius no longer can be labeled V_t or V_r . Also, in general, Doppler velocity values contain a contribution from storm motion and environmental winds. So in order to obtain a representative peak Doppler velocity (V_d) value, a mean peak value can be computed:

$$V_d = \frac{V_d(+) - V_d(-)}{2} \quad (11)$$

where $V_d(+)$ is the more positive (less negative) peak value and $V_d(-)$ is the more negative (less positive) peak value.

Substituting Eq. (11) into (7) and (8) and adding the appropriate trigonometric functions, we find that

$$\zeta = \frac{2\bar{V}_d \cos \theta}{R} \quad (12)$$

$$\vec{V} \cdot \vec{V} = \frac{2\bar{V}_d \sin \theta}{R} \quad (13)$$

where ζ represents the amount of pattern rotation from the pure mesocyclone position shown in Fig. 3; counterclockwise rotation is positive. Cyclonic vorticity ($\zeta > 0$) is a maximum when $\theta = 0^\circ$; anticyclonic vorticity ($\zeta < 0$) reaches a peak when $\theta = 180^\circ$; divergence ($\vec{V} \cdot \vec{V} > 0$) reaches a maximum when $\theta = 90^\circ$; convergence ($\vec{V} \cdot \vec{V} < 0$) is a peak when $\theta = 270^\circ$.

When a vertical distribution of divergence is available, vertical velocity (w) within the core region can be computed. The procedure is to use the mass continuity equation

$$\vec{V} \cdot \vec{V} + \frac{\partial w}{\partial z} - kw = 0 \quad (14)$$

where k is the logarithmic decrease of density with height (can be approximated using a constant value of 0.1 km^{-1} -- e.g., Kessler (14)). Put into finite difference form, Eq. (14) becomes

$$w_{i+1} = w_i + (kw - \vec{V} \cdot \vec{V}) \Delta z \quad (15)$$

where w is computed at level $i+1$ given w at level i and the mean value of the quantity in parentheses in the vertical $\Delta z (= z_{i+1} - z_i)$ interval. The quantity in parentheses can be expanded by assuming that the parameters vary linearly between the two levels:

$$w'_{i+1} = w'_i (1+\alpha)/(1-\alpha) - [(\vec{V} \cdot \vec{V})_i + (\vec{V} \cdot \vec{V})_{i+1}] \Delta z / (2(1-\alpha)) \quad (16)$$

where α is $k\Delta z/2$. The prime indicates that the vertical velocity values have not been corrected for the cumulative effects of errors in divergence computations. Uncorrected vertical velocities are computed throughout storm depth by assuming that w is zero at the ground (or storm top) and evaluating Eq. (16) at successive Δz steps until storm top (or the ground) is reached. Even though w should return to zero at storm top (or the ground), experience has shown that slightly erroneous divergence values at each Δz step can result in a markedly nonzero final value (e.g., Nelson and Brown (15)).

Uncorrected vertical velocity profiles can be modified by adjusting the values at each level such that w is zero at both the ground and storm top. Adjustment parameters can be computed by adding a vertical velocity error term to the right side of Eq. (16) and evaluating the equation from the ground (storm top) to storm top (ground). Different correction developments are discussed by O'Brien (16), Nelson (17) and Ray *et al.* (18) among others.

3.b. Computation of Vorticity, Divergence and Vertical Velocity

Applying Eqs. (12) and (13) to a single Doppler data set, Fig. 7 shows vertical profiles of vorticity and divergence in a mesocyclone computed from single Doppler velocity signatures. These two profiles seem to be realistic. Low-level convergence topped by divergence at upper levels denotes an updraft. Strongest vorticity (rotation) is found at storm midlevels. Had data extended to storm top, data trends in the two curves suggest that divergence increases toward storm top and vorticity approaches zero.

An uncorrected vertical velocity curve also is shown in Fig. 7. It was computed using Eq. (16), which can be simplified to

$$w'_{i+1} = 1.105263 w'_i - 1.05263 \times 10^3 (\vec{V} \cdot \vec{V})_{i+0.5} \quad (17)$$

when Δz is 1.0 km and the value of the divergence data point at the middle of the Δz interval is used as the interval mean. Computations were made to a height of 9 km. Since the height of storm top was not known, approximate procedures (e.g., Brown and Nelson (19)) could not be employed to produce an adjusted vertical velocity profile.

Single Doppler velocity patterns associated with the type of vertical vorticity and divergence variations found in Fig. 7 are presented in Fig. 8. The modeled patterns (with superimposed streamlines) reflect variations -- at 3 to 5 km intervals from the ground to storm top -- that commonly are seen in mature mesocyclones. A convergent mesocyclone near the ground changes to pure rotation then to a divergent circulation and finally to pure divergence near storm top.

4. DOPPLER RADAR AS A SEVERE STORM SENSOR

In 1971, the National Severe Storms Laboratory (NSSL) commissioned its first of two 10-cm wavelength Doppler radars (Brown *et al.* (20)). Since that time, Doppler radar data have been collected annually in springtime Oklahoma thunderstorms.

By 1975, sufficient single Doppler mesocyclone data -- using Donaldson's criteria -- had been collected to look at basic mesocyclone characteristics (Burgess (21)). During that five year period, 37 mesocyclones were identified; their characteristics are summarized in Table 1. Ninety-five per cent of all mesocyclones had severe weather reported with them and 62% of the mesocyclones were associated with reported tornadoes.

Table 1 reveals no significant differences between mesocyclones that produced tornadoes and those that did not. However, there is a significant difference between those mesocyclones that produce weak tornadoes and those that produce strong tornadoes. The parameter that discriminates between weak and strong tornadoes is mesocyclone tangential velocity or azimuthal shear (tangential velocity difference divided by core diameter -- equal to one-half vorticity for solid rotation). Azimuthal shear associated with strong tornadoes is nearly twice that associated with all other mesocyclones. Three-quarters of mesocyclones producing strong tornadoes had shear values greater than $12 \times 10^{-3} \text{ s}^{-1}$, whereas only 21% of mesocyclones with weak tornadoes and 14% of non-tornadic mesocyclones exceeded that value.

Based on these interesting research results -- including tornado warning lead times of 35 minutes -- the National Weather Service (NWS) wanted to test the mesocyclone identification techniques in an operational setting (Johannessen and Kessler (22)). The Air Weather Service, like NWS, was in need of replacing an aging weather radar network. So the two organizations joined forces with NSSL, the Air Force Geophysics Laboratory (AFGL) and the Federal Aviation Administration to form the Joint Doppler Operational Project (JDOP). NSSL's 10-cm Doppler radar at Norman was chosen as the test facility (Staff (23)).

Table 2 summarizes the results of the JDOP operational tests during 1977 and 1978. Compared are severe weather and tornado warnings issued by the Oklahoma City NWS office with and without the benefit of Doppler information (advisories). Conventional NWS warnings (without Doppler advisories) were based on conventional radar, storm spotter and public reports. About one-half of the conventional NWS warnings were false alarms, whereas only 20% of the mesocyclone-based warnings were not associated with reported damage. Of the severe weather and tornadoes that did occur, half of them were missed using conventional NWS techniques and one-third were not associated with recognized mesocyclone signatures.

The lead time between issuance of a warning (NWS) or advisory (Doppler) and the occurrence of severe (nontornadic) weather during 1978 was the same for both groups. This finding suggests that severe storm radar reflectivity features become evident at about the same time that the Doppler mesocyclone signature has satisfied and time continuity requirements.

Tornado lead time presents a different picture. Conventional NWS tornado warnings had zero lead time on the average, compared to a Doppler lead time of 22 minutes. The problem with conventional NWS tornado warnings is that radar reflectivity patterns do not provide many clues for discriminating between tornadic and nontornadic storms. Most of the help comes from public reports that tornadoes are on the ground -- producing negative lead times. But even this is not much help because over half of the public tornado reports received during JDOP had to be discounted based on damage surveys.

The 22 minute average lead time for tornadoes during the JDOP operation (Table 2) is considerably less than the 35 minute average based on five years of NSSL research results (Table 1). This 13 minute discrepancy easily can be explained. Research data were recorded on computer tapes, so it was possible to trace a mesocyclone signature backward in time to its origin. However, during the real-time operation, a potential mesocyclone signature had to satisfy height and time continuity before an advisory could be issued. The Doppler radar operated using a series of elevated antenna scans that took 6 minutes to complete. Therefore a minimum of 6 minutes was required to establish time continuity. Applying typical mesocyclone characteristics (such as those in Table 1) to Donaldson's criteria, it takes nearly 10 minutes for the average mesocyclone to complete half a rotation. Apparently a second tilt sequence was required on the average -- a total of at least 12 minutes -- before the height and time criteria could be satisfied.

5. CONCLUDING COMMENTS

We have shown from both research findings and operational tests that a single Doppler radar is sufficient for detecting mesocyclones and divergence regions within severe thunderstorms. Furthermore, the addition of single Doppler velocity signature information to the conventional NWS warning procedure during JDOP resulted in several dramatic improvements: (1) the percentage of severe storms for which warnings were issued ($= \text{hits}/(\text{hits} + \text{misses})$) increased from 54 to 70%; (2) the percentage of warnings that verified ($= \text{hits}/(\text{hits} + \text{false alarms})$) jumped from 46 to 80%; and (3) the lead time for issuing

tornado warnings increased from no lead time to over 20 minutes on the average.

Based on the success of JDOP, the three concerned agencies -- National Weather Service, Air Weather Service and Federal Aviation Administration -- continue to move forward with plans to jointly procure a next generation weather radar system (NEXRAD) that incorporates 10-cm Doppler capability (Bonewitz (24)). While the nearly decade-long procurement process continues, scientists within NWS, AFGL and NSSL are developing the many types of computer algorithms that will be needed to compute and display radar derived information for the forecaster's use.

Included among the algorithms are those designed to automatically detect the signatures discussed in this paper. The development of automated signature recognition techniques, however, is complicated by a number of practical problems and considerations. One problem is caused by antenna sidelobes, where strong reflectivity in side lobe can dominate weak reflectivity in the main lobe and Doppler velocity from the side lobe azimuth will appear as if it were measured in the main lobe.

Algorithm development for the NEXRAD Doppler radars has been assured by the choice of 10-cm wavelength for the radars. Radars with wavelengths of 5 cm or less have two serious limitations when used as severe storm detectors: (1) attenuation of the radar signal and (2) limited Doppler velocity interval. The attenuation problem is so grave that a severe storm can disappear from the radar scope when another storm moves between it and the radar. Also, the far edge of a severe storm can disappear, potentially erasing an existing mesocyclone (e.g., Allen *et al.* (25)).

The Doppler velocity problem arises from the fact that, for a given range interval, the measurable Doppler velocity interval decreases with decreasing radar wavelength. Velocities outside the interval (that is, greater in magnitude) "fold" back into the interval as aliased velocities; techniques are available to "unfold" automatically the aliased velocities (e.g., Brown *et al.* (26)). However, for the more severe storms, it commonly is not possible to unscramble real and aliased velocities within the limited velocity intervals of the shorter wavelength radars. Even at 10-cm wavelength, velocity gradients within a storm can be so large that it may be impossible to resolve these problems objectively by computer -- causing false or missed signature recognition.

Even though the computer will play a significant role in the signature recognition process, it merely is relieving operational personnel of some of the more mundane and time-consuming monitoring tasks. Through the use of a judicious human-machine mix, the additional information provided by 10-cm Doppler radars should show a marked improvement in the issuance, accuracy and timeliness of severe weather and tornado warnings.

ACKNOWLEDGMENTS

We appreciate general discussions with Donald Burgess and Dr. Stephan Nelson. Thanks to Alice Adams Krentz for use of the data in Fig. 7 that she prepared for a yet-to-be-published report. Sandra McPherson skillfully typed the manuscript. Figures were drafted expertly by Joan Kimpel and Robert Goldsmith provided additional timely graphics support.

Table 1. Statistics for mesocyclones observed by NSSL Doppler radars from 1971 through 1975. From Burgess (21).

1971-1975 Statistics	All Mesocyclones	Non-tornadic Mesocyclones	All Tornadic Mesocyclones	Weak Tornado Mesocyclones	Strong Tornado Mesocyclones
No. of Mesocyclones	37	14	23	19	4
Peak Tangential Velocity ($m s^{-1}$)	22.3 (13-42)	20.9 (15-25)	23.3 (13-42)	21.5 (13-32)	31.0 (20-42)
Core Diameter (km)	5.7 (2-11)	5.6 (3-11)	5.7 (2-10)	6.0 (4-10)	5.0 (2-10)
Azimuthal Shear ($10^{-3} s^{-1}$)	8.9 (3-20)	8.5 (4-17)	9.1 (3-20)	7.9 (3-13)	15.2 (8-20)
Vertical Extent (km)	7.8 (5-13)	7.8 (5-13)	7.7 (5-11)	7.3 (5-11)	9.5 (8-11)
% With Severe Weather	95	86	100	100	100
% With Tornadoes	62	0	100	100	100
Tornado Lead Time (min)	--	--	35 (13-61)	34 (13-61)	36 (13-58)

() = range of values

Table 2. Summary of 1977-78 JDOP severe weather and tornado warnings. Warnings based on the conventional National Weather Service warning system are compared with those based on mesocyclone signatures detected by Doppler radar. "Hits" are successful warnings, "false alarms" are warnings for storms that did not become severe and "misses" represent severe storms for which no warnings were issued. From Staff (23).

Warning System	Hits	Misses	False Alarms	1978 Severe Weather Lead Time	1977-78 Tornado Lead Time
National Weather Service (Oklahoma City)	104	90 (46%)	123 (54%)	14 min	0 min
Doppler Radar (NSSL, Norman)	70	30 (30%)	17 (20%)	15 min	22 min

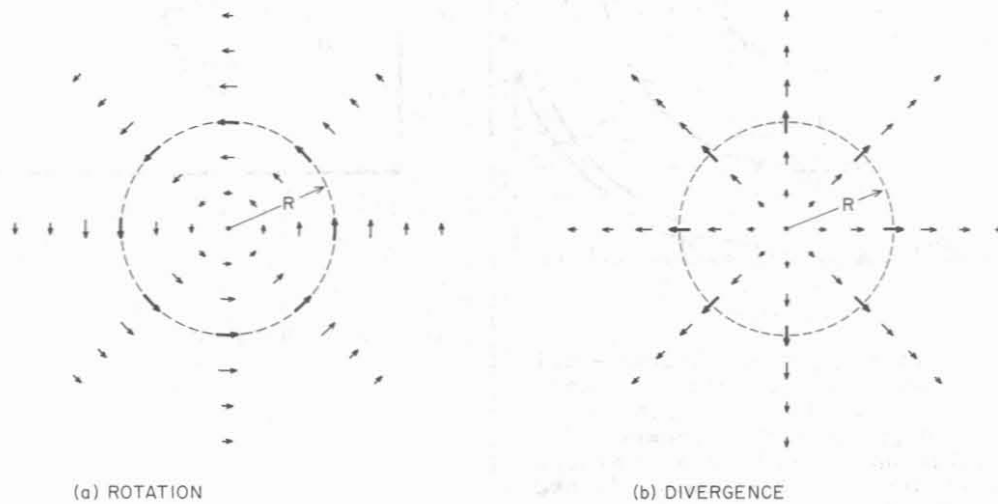


Figure 1. Horizontal flow fields for axisymmetric (a) rotation and (b) divergence. Bold arrows represent maximum velocities at core radius R .

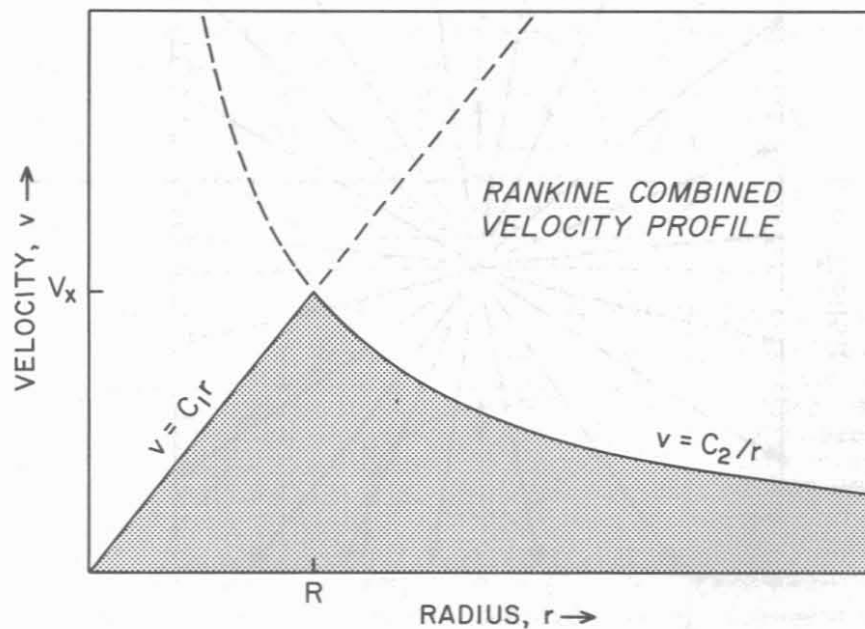


Figure 2. Rankine combined velocity profile, where peak velocity (V_x) is at core radius (R).

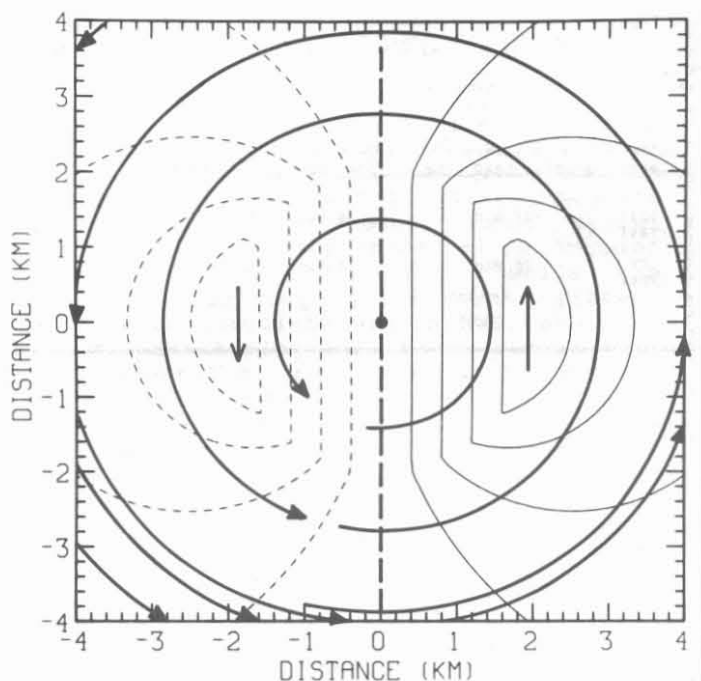


Figure 3. Plan view of mesocyclone model (thick curved lines) and associated single Doppler velocity signature (thin contours). For a Doppler radar located due south of circulation, solid thin contours represent flow away from radar, dashed contours represent flow toward radar.

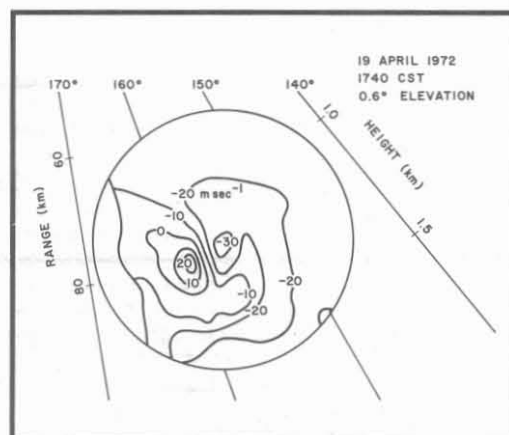


Figure 4. Single Doppler mesocyclone signature in the Davis, OK tornadic storm on 19 April 1972. Radar is located beyond upper left corner of figure; flow away from radar is positive, toward is negative. From Burgess (11).

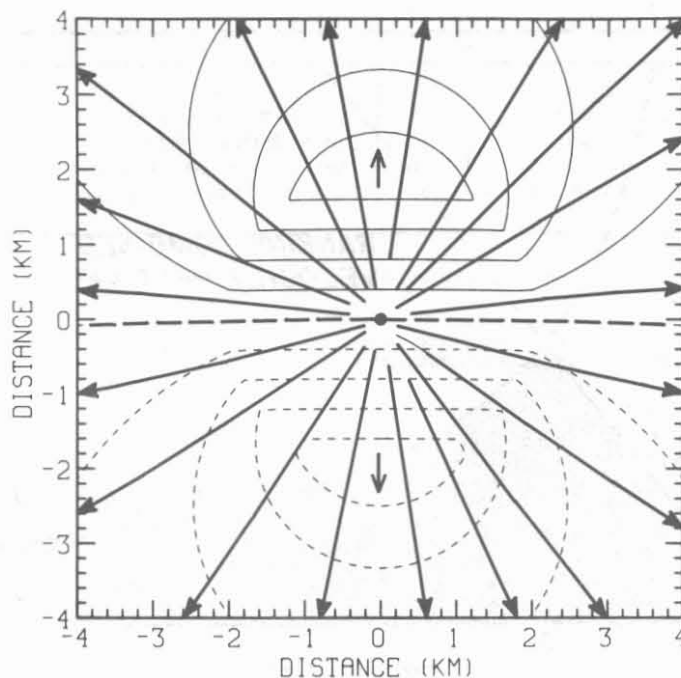


Figure 5. Plan view of axisymmetric divergence model (thick radial lines) and associated single Doppler velocity signature (thin contours). For a Doppler radar located due south of the divergence area, solid thin contours represent flow away from radar, dashed contours represent flow toward radar.

30 MAY 1976
1616 CST

14 km AGL

130 km —

140 —

150 —

160 —

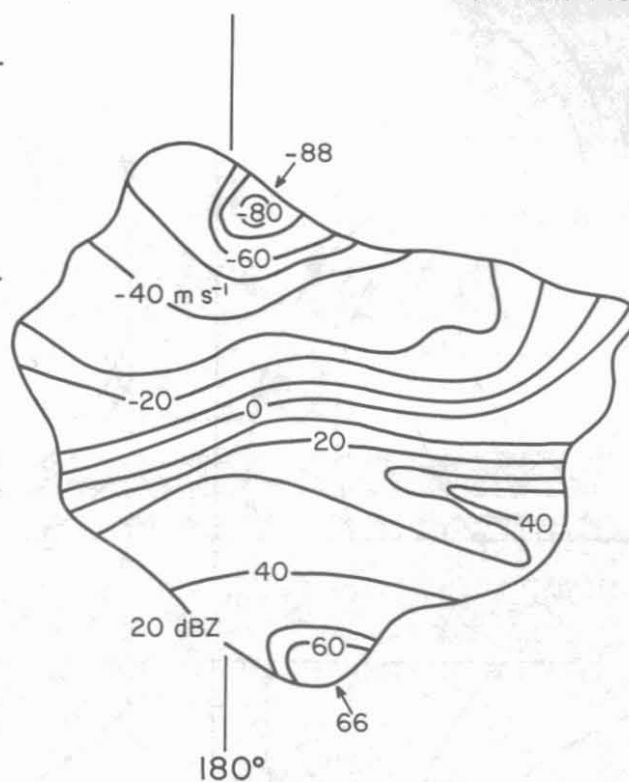


Figure 6. Single Doppler divergence signature near the top of the Waurika, OK tornadic storm on 30 May 1976. Radar is located above the top of figure (180° azimuth direction is indicated). Measured Doppler velocities are positive for flow away from radar, negative for flow toward radar. From Lemon and Burgess (12).

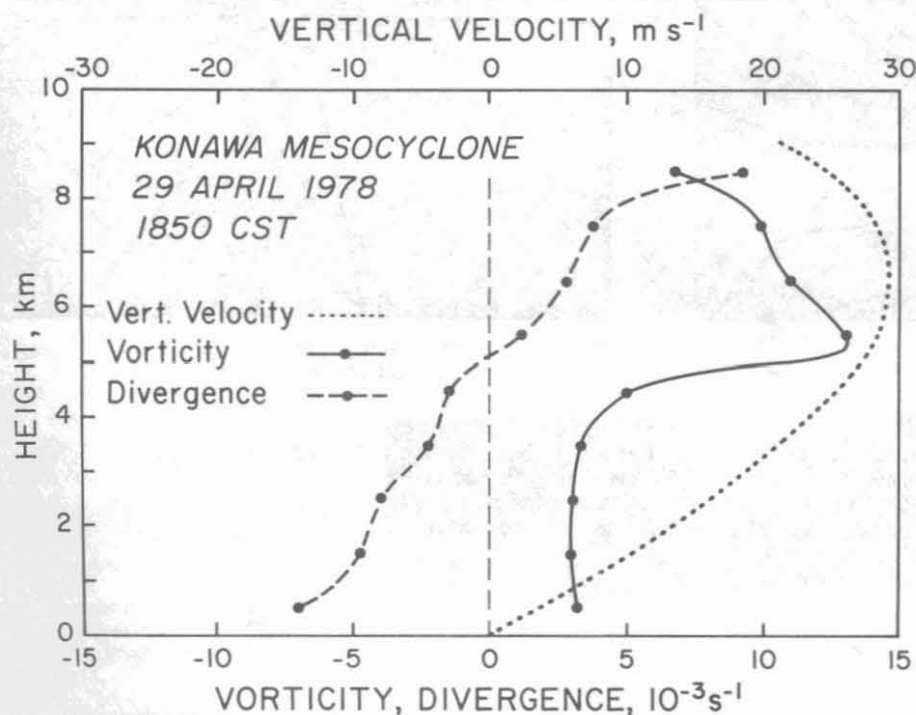


Figure 7. Vertical profiles of vorticity, divergence and uncorrected vertical velocity for the mesocyclone in the Konawa right-moving severe storm on 29 April 1978. Profiles were computed from single Doppler velocity data using Eqs. (12), (13) and (17). Data courtesy of Alice Adams Krentz.

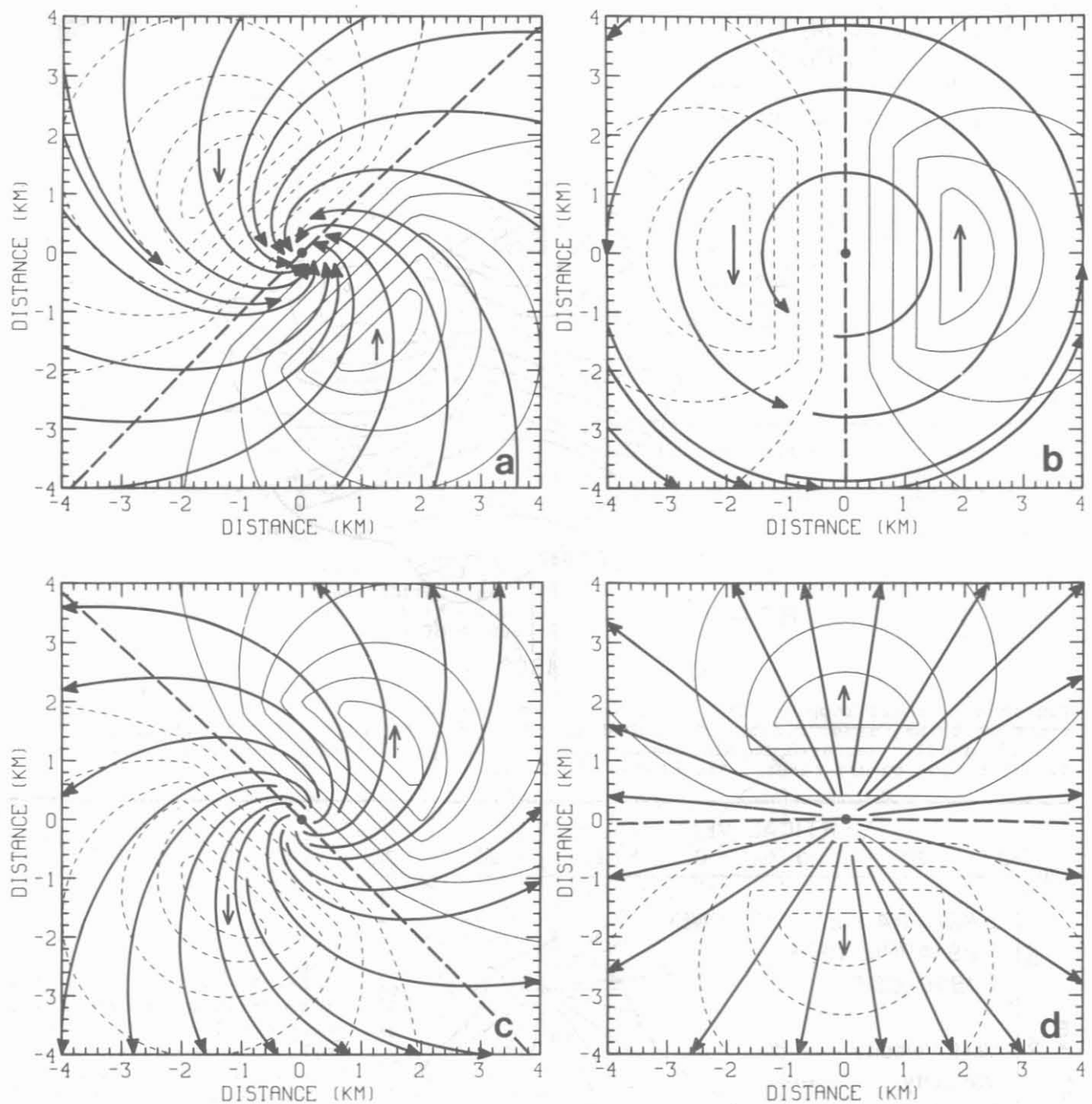


Figure 8. Modeled single Doppler velocity patterns (thin contours) and equivalent horizontal flow fields (thick curves) at 3 to 5 km height intervals in a typical severe storm. The patterns represent (a) convergent rotation near the ground, (b) pure rotation at lower midlevels, (c) divergent rotation at upper midlevels, (d) pure divergence near storm top.

REFERENCES AND FOOTNOTES

1. Rodger A. Brown is a research meteorologist at the National Severe Storms Laboratory. He received a B.S. degree from Antioch College, a M.S. degree from the University of Chicago and is continuing graduate studies at the University of Oklahoma. His research interests are in severe storms and meso-meteorology, utilizing Doppler radar as a primary data source.
2. Vincent T. Wood is a research meteorologist at the National Severe Storms Laboratory. He received a B.A. degree from the University of St. Thomas, a M.S. degree from Texas A&M University and is continuing graduate studies at the University of Oklahoma. His research interests are meteorological modeling, severe storms, and mesocyclone and tornado dynamics.
3. Grebe, R., 1981: Operational Doppler radar -- is it worth it? Nat. Wea. Digest, 6, 48-52.
4. Easterbrook, C. C., 1967: Some Doppler radar measurements of circulation patterns in convective storms. J. Appl. Meteor., 6, 882-888.
5. Donaldson, R. J., Jr., 1967: Horizontal wind measurement by Doppler radar in a severe squall line. Preprints, Fifth Conf. on Severe Local Storms (St. Louis), Boston, Amer. Meteor. Soc., 89-98.
6. Peace, R. L., Jr., and R. A. Brown, 1968: Comparison of single and double Doppler radar velocity measurements in convective storms. Preprints, Thirteenth Radar Meteor. Conf. (Montreal), Boston, Amer. Meteor. Soc., 464-473.
7. Donaldson, R. J., Jr., G. M. Armstrong, A. C. Chmela and M. J. Kraus, 1969: Doppler radar investigation of air flow and shear within severe thunderstorms. Preprints, Sixth Conf. on Severe Local Storms (Chicago), Boston, Amer. Meteor. Soc., 146-154.
8. Lhermitte, R. M., 1969: Doppler radar observation of a convective storm. Preprints, Sixth Conf. on Severe Local Storms (Chicago), Boston, Amer. Meteor. Soc., 139-145.
9. Donaldson, R. J., 1970: Vortex signature recognition by Doppler radar. J. Appl. Meteor., 9, 661-670.
10. Rankine, W.J.M., 1901: A Manual of Applied Mechanics, 16th edition. London, Charles Griff and Company, 574, 578.
11. Burgess, D. W., 1974: Study of a severe right-moving thunderstorm utilizing new single Doppler radar evidence. M. S. thesis, Dept. of Meteorology, Univ. of Oklahoma, 77 pp.
12. Lemon, L. R., and D. W. Burgess, 1980: Magnitude and implications of high speed outflow at severe storm summits. Preprints, Nineteenth Conf. on Radar Meteor. (Miami), Boston, Amer. Meteor. Soc., 364-368.
13. Spiegel, M. R., 1959: Vector Analysis and An Introduction to Tensor Analysis, New York, Schaum Publishing Co., 225 pp.
14. Kessler, E., 1969: On the distribution and continuity of water substance in atmospheric circulation. Meteor. Monographs, 10 (32), 84 pp.
15. Nelson, S. P., and R. A. Brown, 1982: Multiple Doppler radar derived vertical velocities in thunderstorms. Part I - Error analysis and solution techniques. NOAA Tech. Memo. ERL NSSL-94, Norman, Nat. Severe Storms Lab., 1-10. (Available from National Technical Information Service, Springfield, VA 22151 as PB83-152553.)
16. O'Brien, J. J., 1970: Alternate solutions to the classical vertical velocity problem. J. Appl. Meteor., 9, 197-203.
17. Nelson, S. P., 1980: A study of hail production in a supercell storm using a Doppler derived wind field and a numerical hail growth model. NOAA Tech. Memo. ERL NSSL-89, Norman, Nat. Severe Storms Lab., 90 pp. (Available from National Technical Information Service, Springfield, VA 22151 as PB81-17822Q.)
18. Ray, P. S., C. L. Ziegler, W. Bumgarner and R. J. Serafin, 1980: Single- and multiple-Doppler radar observations of tornadic storms. Mon. Wea. Rev., 108, 1607-1625.
19. Brown, R. A., and S. P. Nelson, 1982: Multiple Doppler radar derived vertical velocities in thunderstorms. Part II - Maximizing a real extent of vertical velocities. NOAA Tech. Memo. ERL NSSL-94, Norman, Nat. Severe Storms Lab., 11-21. (Available from National Technical Information Service, Springfield, VA 22151 as PB83-152553.)
20. Brown, R. A., W. C. Bumgarner, K. C. Crawford and D. Sirmans, 1971: Preliminary Doppler velocity measurements in a developing radar hook echo. Bull. Amer. Meteor. Soc., 52, 1186-1188.
21. Burgess, D. W., 1976: Single Doppler radar vortex recognition: Part I - Mesocyclone signatures. Preprints, Seventeenth Conf. on Radar Meteor. (Seattle), Boston, Amer. Meteor. Soc., 97-103.
22. Johannessen, K., and E. Kessler, 1976: Program to develop Doppler for use in the National Weather Service. Preprints, Seventeenth Conf. on Radar Meteor. (Seattle), Boston, Amer. Meteor. Soc., 560-561.
23. Staff, NSSL, AFGL, NWS, AWS, 1979: Final report on the Joint Doppler Operational Project (JDOP), 1976-1978. NOAA Tech. Memo. ERL NSSL-86, Norman, Nat. Severe Storms Lab., 84 pp. (Available from National Technical Information Service, Springfield, VA 22151 as PB80-107188/AS.)
24. Bonewitz, J. D., 1981: The NEXRAD program -- An overview. Preprints, Twentieth Conf. on Radar Meteor. (Boston), Boston, Amer. Meteor. Soc., 757-761.
25. Allen, R. H., D. W. Burgess and R. J. Donaldson, Jr., 1981: Attenuation problems associated with a 5 cm. radar. Bull. Amer. Meteor. Soc., 62, 807-810.
26. Brown, R. A., C. R. Safford, S. P. Nelson, D. W. Burgess, W. C. Bumgarner, M. L. Weible and L. C. Fortner, 1981: Multiple Doppler radar analysis of severe thunderstorms: Designing a general analysis system. NOAA Tech. Memo. ERL NSSL-92, Norman, Nat. Severe Storms Lab., 21 pp. (Available from National Technical Information Service, Springfield, VA 22151 as PB82-114117.)